RESEARCH FRONT

CSIRO PUBLISHING

Aust. J. Chem. **2017**, *70*, 478–484
http://dx.doi.org/10.1071/CH16547

Full Paper

Synthesis and Structures of Rare Earth 3-(4′-Methylbenzoyl)-propanoate Complexes – New Corrosion Inhibitors*

Caspar N. de Bruin-Dickason,[A] *Glen. B. Deacon,*[A,D] *Craig M. Forsyth,*[A] *Schirin Hanf,*[A] *Oliver B. Heilmann,*[A] *Bruce R. W. Hinton,*[B] *Peter C. Junk,*[C,D] *Anthony E. Somers,*[B] *Yu Qing Tan,*[A] *and David R. Turner*[A]

[A]School of Chemistry, Monash University, Clayton, Vic. 3800, Australia.
[B]Institute for Frontier Materials, Deakin University, Geelong, Vic. 3220, Australia.
[C]College of Science and Engineering, James Cook University, Townsville, Qld 4811, Australia.
[D]Corresponding authors. Email: glen.deacon@monash.edu; peter.junk@jcu.edu.au

A series of rare earth 3-(4′-methylbenzoyl)propanoate (mbp^-) complexes $[RE(mbp)_3(H_2O)]$ (RE = rare earth = Y, La, Ce, Nd, Ho, Er) have been prepared by either metathesis reactions between the corresponding rare earth chloride and Na(mbp) or protolysis of rare earth acetates by the free acid. Single-crystal X-ray diffraction studies of $[RE(mbp)_3(H_2O)]$ (RE = Ce, Nd) and $[Ce(mbp)_3(dmso)]$ reveal a 1D carboxylate-bridged polymeric structure in the solid state, featuring 9-coordinate rare earth ions. X-ray powder diffraction patterns of the bulk materials indicates that all of the $[RE(mbp)_3(H_2O)]$ complexes except RE = La are isomorphous. Hence, there is no structural change from the complex with RE = Ce to that with RE = Er despite the lanthanoid contraction. The ^1H NMR spectra of the RE = Ho or Er complexes in $(CD_3)_2SO$ show large paramagnetic shifts and broadening of the CH_2 resonances, indicating the retention of substantial carboxylate coordination in solution.

Manuscript received: 29 September 2016.
Manuscript accepted: 17 October 2016.
Published online: 15 November 2016.

Introduction

Chemical corrosion inhibitors play a major role in reducing the multi-billion dollar cost of corrosion of metal (particularly steel) infrastructure.[1] For many years, metal chromates were dominant in this role.[1a,2] However, concerns over their toxicity[3] are driving the phasing out of their use and a search for more benign replacements.[1a,2] In this context, rare earth salts show significant anti-corrosion activity[4] and are environmentally friendly, as shown by their widespread use in agriculture in China[5] and by their use as feedstock additives in Switzerland.[6] Because arene-functionalised carboxylate ions can also show anti-corrosion properties, albeit at higher concentrations,[7] we are examining the inhibitor properties of rare earth carboxylate complexes, particularly for steel (see Fig. 1 for examples of carboxylate ions of interest).[2]

For example, lanthanoid salicylates (Ligand A, Fig. 1) are effective inhibitors with the cerium complex being the best performer.[7] Additionally, there has been success in preparing Fe/Ce salicylate bimetallics that model the protective film on steel.[8] From a wide range of rare earth cinnamates[9] and substituted cinnamates,[10] lanthanum 4-hydroxycinnamate (Ligand B, Fig. 1) is the optimum performer.[11] In certain applications, the praseodymium complex performs well.[12] In developing an understanding of structural features favouring inhibition, it has been shown that lanthanum 3-(4′-hydroxyphenyl)propanoate (Ligand C, Fig. 1) is much less effective than lanthanum 4-hydroxycinnamate, thereby establishing the importance of the cinnamate double bond in corrosion inhibition.[13] Rare earth 3-(4′-methylbenzoyl)propanoate (mbp)

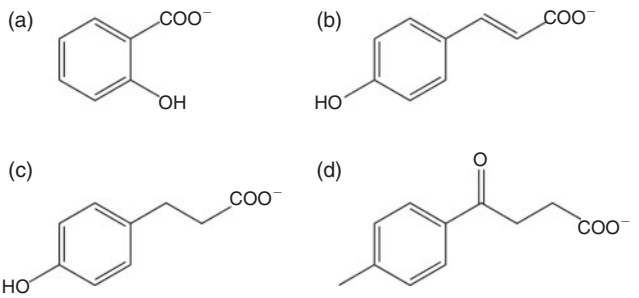

Fig. 1. Carboxylate anions used in the present and previous studies: (a) 2-hydroxybenzoate (salicylate ($Hsal^-$)); (b) 4-hydroxycinnamate (4-OH-$cinn^-$); (c) 3-(4′-hydroxyphenyl)propanoate (hpp^-); (d) 3-(4′-methylbenzoyl)propanoate (mbp^-).

*This paper is dedicated to our colleague and friend Professor Len Lindoy on the occasion of his 80th birthday.

(4-(4′-methylphenyl)-4-oxobutanoate) (Ligand D, Fig. 1) complexes are now a current focus, as the parent acid has been a commercial inhibitor supplied by Ciba as Irgacor 419. It is currently available as a 2 : 1 mixture with 4-ethylmorpholine as Irgacor1405. Iron complexes modelling the behaviour of mbp^- on an iron surface have been published.[14] We now report the preparation and structures of rare earth (RE) 3-(4′-methylbenzoyl)propanoate complexes $[RE(mbp)_3(H_2O)]$ (RE = Y, La, Ce, Nd, Ho and Er) and $[Ce(mbp)_3(dmso)]$. Preliminary reports on their anti-corrosion behaviour have been given.[15] The choice of rare earth elements covers virtually the whole size range and includes some paramagnetic ions for exploring solution behaviour.

Results and Discussion

The synthesis of $[RE(mbp)_3(H_2O)]$ complexes was accomplished by two methods. Metathesis reactions between three molar equivalents of the sodium salt Na(mbp) either isolated or prepared in situ and the required hydrated rare earth chloride yielded the desired complexes in high yields as a colourless (RE = Y, La, Ce, Nd) or light pink (RE = Ho, Er) microcrystalline solids (Scheme 1a). These complexes could also be prepared in similar yields through protolysis reactions between the free carboxylic acid and the corresponding rare earth acetate (Scheme 1b). The bulk products were obtained analytically pure (C, H, RE). Results of the thermogravimetric analysis (TGA) indicated the loss of one coordinated water in the range of 80–130°C (the mass loss was lower than 1 H_2O for the complex with RE = La) and gradual decomposition after 230°C.

Structural Studies

Single crystals of $[RE(mbp)_3(H_2O)]$ (RE = Ce, Nd) were grown from filtrates of the synthesis reaction mixtures after standing for several months, single crystals of $[Ho(mbp)_3(H_2O)]$ were obtained from an H-tube synthesis (see *Experimental*), and single crystals of $[Ce(mbp)_3(dmso)]$ were grown from a saturated dmso solution over several weeks. In contrast, obtaining single crystals of the other $[RE(mbp)_3(H_2O)]$ complexes has been unsuccessful thus far.

The X-ray data for $[RE(mbp)_3(H_2O)]$ (RE = Ce, Nd, Ho) and $[Ce(mbp)_3(dmso)]$ were solved in $P2_1/c$ (No. 14) and $C2/c$ (No. 15) space groups, respectively, with one formula unit in the asymmetric unit. The structures are depicted in Fig. 2, and selected bond lengths are presented in Table 1. Data for the holmium complex were of sufficient quality to only establish connectivity, and thus the bond lengths of this complex are not discussed. These complexes have a similar 1D polymeric structure (Fig. 2). Each structure features 9-coordinate lanthanoid ions terminally bound by one aqua (or O-dmso, as consistent with the hard acid nature of the Ce^{3+} ion) ligand, and six bridging mbp ligands. In $[RE(mbp)_3(H_2O)]$ and $[Ce(mbp)_3(dmso)]$ complexes, RE1 is bound by one oxygen atom

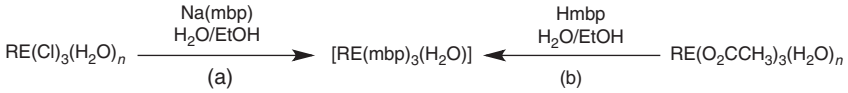

Scheme 1. Preparation of the $[RE(mbp)_3(H_2O)]$ complexes.

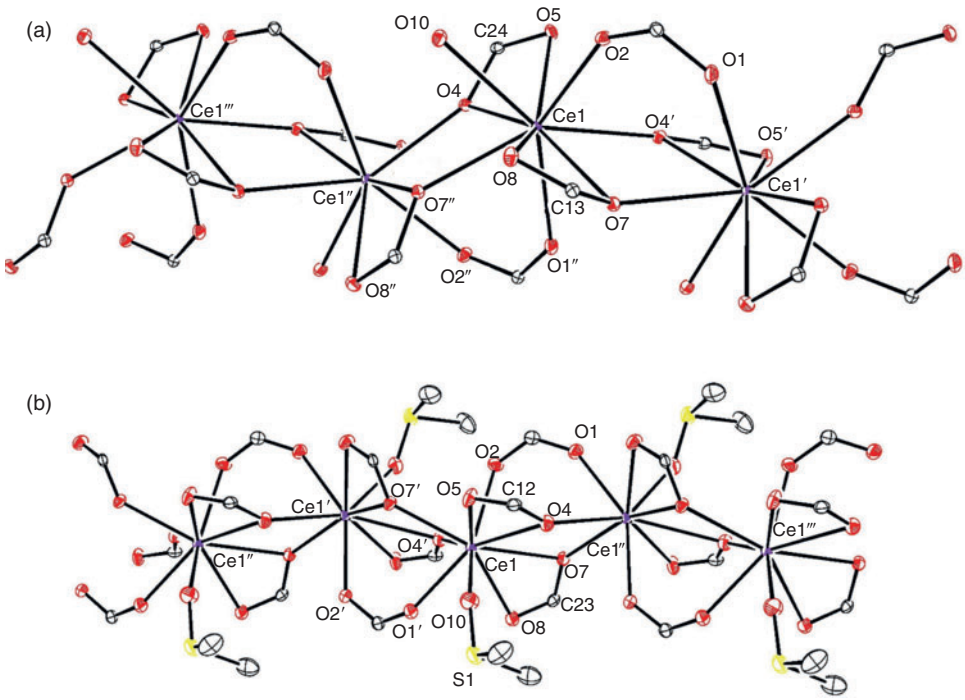

Fig. 2. Extended 1D chain of (a) $[Ce(mbp)_3(H_2O)]_n$ and (b) $[Ce(mbp)_3(dmso)]_n$ showing the coordination sphere around the Ce^{3+} metal ions and connectivity to symmetrically equivalent cerium atoms. Carboxylate ligands are truncated for clarity.

from each of the two μ-1κ(O):2κ(O′) ligands (O2, O1″ to Ce1 (Fig. 2a)), both oxygen atoms from two μ-1κ(O,O′):2κ(O′) ligands (O4, O5, O7, O8 to Ce1 (Fig. 2a)), and one oxygen atom from each of the two μ-1κ(O′):2κ(O,O′) ligands (O7″, O4′ to Ce1 (Fig. 2a)). Although the dmso analogue has a similar coordination arrangement (Fig. 2b), the two mbp ligands chelating to Ce1 both bridge to the same cerium atom. In contrast, in the aqua complex, these ligands bridge to different Ce atoms. The structural difference is best illustrated by the angle subtended by the carboxylate carbons of the chelating carboxylate groups at RE1, namely *transoid* for the aqua complexes (169.2(1)° (RE = Ce); 169.1(2)° (RE = Nd)) and *cisoid* (105.545(5)°) for the dmso complex. The benzoyl carbonyl groups do not interact with the RE atoms with RE–O(3) distances of ≥6.0 Å. Hydrogen bonding is observed between an aqua hydrogen and a carboxyl oxygen with O10—O1′ distances of 2.762(4) Å for the Ce complex and 2.765(6) Å for Nd.

Table 1. Bond lengths (Å) and angles (°) in [RE(mbp)$_3$(solv)] complexes

	Ce(mbp)$_3$(dmso)	Ce(mbp)$_3$(H$_2$O)	Nd(mbp)$_3$(H$_2$O)
Ln1–O1′	2.457(2)	2.537(4)	2.488(6)
Ln1–O2	2.449(2)	2.430(3)	2.392(6)
Ln1–O4′	2.473(2)	2.527(3)	2.492(6)
Ln1–O4	2.751(2)	2.580(3)	2.556(6)
Ln1–O5	2.516(2)	2.656(3)	2.616(6)
Ln1–O7	2.699(2)	2.542(3)	2.505(6)
Ln1–O7′	2.538(2)	2.422(3)	2.407(6)
Ln1–O8	2.587(2)	2.551(3)	2.530(6)
Ln1–O10	2.513(2)	2.490(3)	2.448(3)
Ln1–Ln1′	4.3450(2)	4.1305(8)	4.0865(8)
C12–Ce1–C23	105.545(5)	–	–
C1–Ln1–C12	–	169.235(4)	169.1(2)

The larger < Ce–O > bond length in the dmso complex when compared with that in the aqua analogue may be attributed to the greater bulk of the neutral ligand.[16] The [Nd(mbp)$_3$(H$_2$O)] complex features a slightly shorter average Nd–O bond length of 2.49 Å, when compared with the cerium analogue (2.525 Å), as consistent with the difference in the 9-coordinate ionic radii.[17] The RE–OC(O)R bond lengths show considerable variation with the average value approximately 0.05 Å greater than RE–OH$_2$ or Ce–OSMe$_2$ in the respective complexes despite the ligand charge. Overall, the < RE–O > bond lengths of the aqua complexes are in excellent agreement with the corresponding values of Ce or Nd atoms of the same coordination numbers in [Ce$_2$(hpp)$_6$(H$_2$O)$_3$] and [NaNd(hpp)$_7$(H$_2$O)(MeOH)][13] complexes, where the mbp chain can be viewed as a functionalised hpp (Ligand C, Fig. 1).

Powder X-ray diffraction (XRD) data from bulk samples of the [RE(mbp)$_3$(H$_2$O)] (RE = Y, Ce, Nd, Ho, Er) complexes indicate that they are isomorphous and match the calculated patterns of the [RE(mbp)$_3$(H$_2$O)] (RE = Ce, Nd) structures (Fig. 3). Slight differences between the experimental and simulated patterns are attributable to the considerable temperature difference between the powder XRD and single-crystal measurements. The lanthanum complex shows a significantly different pattern and thus evidently adopts a different structure in the solid state, possibly due to the larger ionic radius of La^{3+} when compared with those of the other rare earth metals.[17] For example, a change in the coordination of a μ-1κ(O):2κ(O′) ligand to μ-1κ(O,O′):2κ(O′) would enable 10-coordination to be attained within the 1D polymer. A structural change from La to Ce (ionic radius difference of 0.025 Å)[17] is unusual but not unknown e.g. for [LnCl$_3$(thf)$_2$][18] and [Ln(Odpp)$_3$] (Odpp = 2, 6-diphenylphenolate).[19] The structural conformity from Ce to Er is in stark contrast to previously synthesised lanthanoid carboxylate corrosion inhibitors bearing anthranilate,[20]

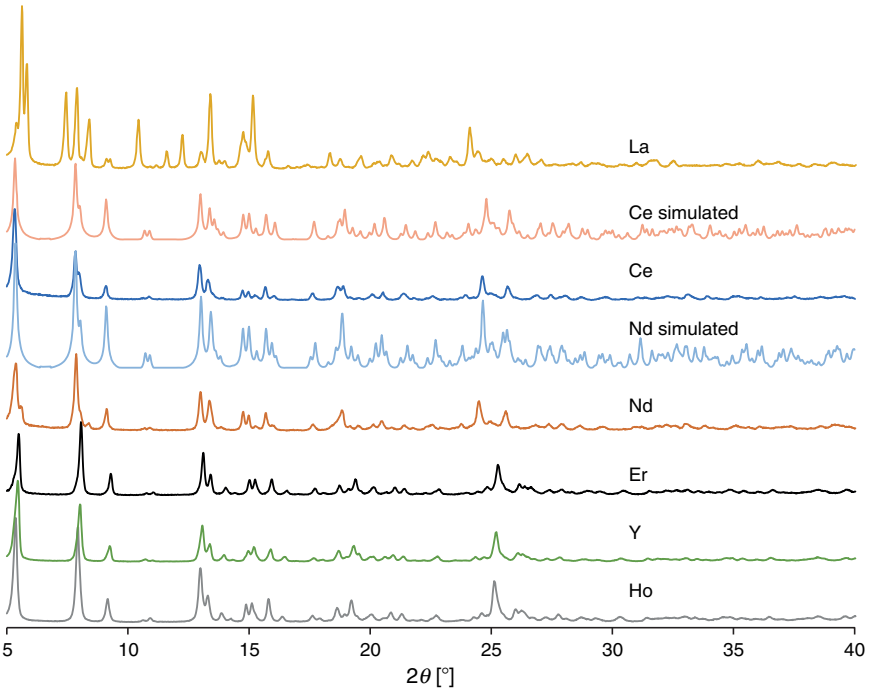

Fig. 3. Powder XRD data of bulk samples of the [RE(mbp)$_3$(H$_2$O)] complexes and simulated powder XRD patterns obtained from [RE(mbp)$_3$(H$_2$O)] single crystal data.

cinnamate,[9,10] and salicylate ligands,[21] which show significant structural variation across the lanthanoid series.

Infrared (IR) Spectra

The key features of the IR spectra of the $[RE(mbp)_3H_2O]$ complexes are given in Table 2. For the isostructural series $[RE(mbp)_3(H_2O)]$ (RE = Y, Ce, Nd, Ho, Er), data are given only for RE = Ce as the compounds are isospectral (Fig. S1, Supplementary Material). Data for $[La(mbp)_3(H_2O)]$ differ somewhat from those of the isostructural series, as is consistent with the structural difference indicated by X-ray powder data. All complexes show the expected features with ν_s(C=O) of the carbonyl not shifted significantly from the sodium salt value, as is consistent with the lack of carbonyl–metal interactions in the structures. In addition, the $\nu_{as}(CO_2)$ and $\nu_s(CO_2)$ bands of the complexes do not differ much from the values for the sodium salt, consistent with bridging carboxylates,[22] whereas the splitting may reflect the two bridging modes.

NMR Spectra

As complexes with both diamagnetic and paramagnetic rare earth ions are available, comparison of their ^{1}H and ^{13}C NMR spectra can provide information on whether the carboxylate ligands are displaced by donor solvents in solution. Table 3 provides chemical shifts of the methylene groups, which are nearest to the RE^{3+} ion, and the methyl groups, which are the most distant from the RE^{3+} ion. Similar spectra of both diamagnetic and paramagnetic analogues would be indicative of substantial carboxylate displacement. In [D6]dmso, the paramagnetic Ce, Nd, Ho, and Er complexes show major broadening and considerable shifts of the methylene resonances from the values of the diamagnetic complexes (Table 3), as is consistent with the maintenance of carboxylate coordination in solution. However, the methyl resonance shows minimal broadening and smaller shifts from the diamagnetic analogues. Additionally, in the ^{13}C NMR spectra of the Ce and Nd complexes, the signals for the carboxylate carbon and α-methylene carbon are absent in the 0–250 ppm range, probably due to paramagnetic broadening, whereas other signals appear at similar values observed for the diamagnetic analogues. Isolation of $[Ce(mbp)_3(dmso)]$ from dissolution of the aqua complex in dmso also suggests retention of mbp ligation in solution. Paramagnetic shifting was less pronounced for the Ho and Er complexes in D_2O, implying significant displacement of the mbp ligands by water. However, the complexes have low solubility in D_2O, necessitating ultrasonication and heating to obtain sufficient concentration in solution for a detectable signal, potentially assisting ligand dissociation.

Table 2. Selected infrared bands (cm^{-1}) of the $[RE(mbp)_3(H_2O)]$ complexes

Complex	$\nu(OH)_{water}$	ν_s(C=O)	$\nu_{as}(CO_2)$	$\nu_s(CO_2)$
Na(mbp)	3346, 3235	1683	1559	1399
$[La(mbp)_3(H_2O)]$	3514, 3463	1681, 1667	1576, 1550, 1526	1435, 1406
$[Ce(mbp)_3(H_2O)]$	3455	1692, 1674	1572, 1542	1423, 1400

Table 3. Selected ^{1}H chemical shifts (ppm) of the 3-(4′-methylbenzoyl) propanoate complexes in different solvents

	$(CD_3)_2SO$			D_2O		
	CH_2CO_2	CH_2CO	CH_3	CH_2CO_2	CH_2CO	CH_3
Na(mbp)	2.34	3.10	2.34	2.60	3.36	2.48
$[Y(mbp)_3(H_2O)]$	2.39	3.11	2.35	2.52	3.27	2.37
$[La(mbp)_3(H_2O)]$	2.39	3.09	2.35	–	–	–
$[Ce(mbp)_3(H_2O)]$	3.95	3.95	2.42	–	–	–
$[Nd(mbp)_3(H_2O)]$	4.35	4.35	2.39	–	–	–
$[Ho(mbp)_3(H_2O)]$	29.9	17.2	2.83	3.47	3.76	2.46
$[Er(mbp)_3(H_2O)]$	−2.63	−0.13	2.04	2.26	3.15	2.38

Conclusions

Six new rare earth 3-(4′-methylbenzoyl)propanoate complexes have been synthesised through either metathesis or protolysis pathways in high yields and characterised by NMR and IR spectroscopy, powder XRD, TGA, microanalyses, and metal analyses. The ^{1}H and ^{13}C NMR spectra of these complexes suggest that coordination of the carboxylate ligands is maintained in dmso solution. Additionally, X-ray crystallographic examination of single crystals of $[RE(mbp)_3(H_2O)]$ (RE = Ce, Nd, Ho) and the dmso-coordinated analogue, $[RE(mbp)_3(dmso)]$, revealed a 1D polymeric structure for the complexes with 9-coordinate RE^{3+} ions. The powder XRD and IR data suggest that the polymeric structure of $[RE(mbp)_3(H_2O)]$ complexes is the same for RE = Y, Ce, Nd, Ho, Er, but the lanthanum analogue adopts a different structure in the solid state. Investigation of the potential application of the prepared complexes as corrosion inhibitors and the mechanism through which they inhibit corrosion is ongoing.[15] The evidence from the NMR data that carboxylate coordination persists in solution is particularly relevant. To fully determine the role of the structures on inhibiting corrosion, a complete study is required on the influence of the RE on the anti-corrosion behaviour of the mbp complexes.

Experimental

General

IR spectra were collected as solid samples using an Agilent Cary 630 attenuated total reflectance (ATR-IR) spectrometer between 4000 and 600 cm^{-1}. ^{1}H and ^{13}C NMR spectra were recorded on either a Bruker DPX300 or a Bruker Avance III 400 spectrometer, and chemical shifts were referenced to the residual ^{1}H resonances of the deuterated solvents. Melting points were determined in glass capillaries and are reported uncalibrated. Microanalyses were performed by either the Campbell Microanalytical Service of the University of Otago (New Zealand) or the Elemental Analysis Service of London Metropolitan University (UK). Metal analyses were performed by titration of HCl-digested samples against Na_2H_2EDTA in hexamine-buffered solution with Xylenol orange indicator. TGA was performed on a Mettler Toledo TGA-DSC1 instrument using standard 40 μL Al metal pans in the temperature range of 35–400°C (with a ramp of 5°C min^{-1}) under nitrogen gas flow (30 mL min^{-1}). Powder XRD measurements were performed at room temperature on a Bruker D8 ADVANCE Eco fitted with a Lynxeye detector using Cu radiation (wavelength = 1.54059 Å) with a Ni filter.

Na(mbp)

3-(4′-Methylbenzoyl)propanoic acid (0.89 g, 4.7 mmol) was neutralised with sodium hydrogen carbonate (0.39 g, 4.7 mmol) in a mixture of ethanol (EtOH) and water (1 : 1 v/v). Upon

evaporation of solvent under a gentle stream of air, Na(mbp) was recovered as a colourless solid (0.99 g, 99 %), mp 196–198°C. ν_{max} (neat)/cm^{-1} 3058wbr, 2920wbr, 1683s, 1560s, 1400s, 1357s, 1268m, 1197m, 1179m, 1151m, 982m br, 765s. δ_H ([D$_6$]dmso, 400.17 MHz) 2.31 (2H, t, C*H*$_2$COO), 2.34 (3H, s, C*H*$_3$), 3.10 (2H, t, C*H*$_2$CO), 7.27 (2H, d, Ar *m-H*), 7.84 (2H, d, Ar *o-H*). δ_H ([D$_2$O], 400.17 MHz) 2.31 (3H, s, C*H*$_3$), 2.61 (2H, t, C*H*$_2$COO), 3.36 (2H, t, C*H*$_2$CO), 7.44 (2H, d, Ar *m-H*), 7.96 (2H, d, Ar *o-H*). δ_C([D$_6$]dmso, 75 MHz) 32.3, 35.5, 128.0, 129.2, 134.7, 143.0, 177.0, 200.0.

K(mbp)

3-(4′-Methylbenzyol)propanoic acid (0.96 g, 4.9 mmol) was neutralised with potassium carbonate (0.34 g, 2.4 mmol) in a mixture of EtOH and water (1 : 1 v/v). Upon evaporation of solvent under a gentle stream of air, K(mbp) was recovered as a colourless solid (0.99 g, 99 %). ν_{max} (neat)/cm^{-1} 3354w br, 2920wbr, 1678s, 1562s, 1398s, 1357m, 1248m, 1182m, 970mbr, 812s, 793s. δ_H ([D$_2$O], 400.17 MHz) 2.43 (3H, s, C*H*$_3$), 2.69 (2H, t, C*H*$_2$COO), 3.37 (2H, t, C*H*$_2$CO), 7.42 (2H, d, Ar *m-H*), 7.97 (2H, d, Ar *o-H*).

[Y(mbp)$_3$(H$_2$O)]

A freshly prepared solution of Na(mbp) (0.21 g, 0.98 mmol) in 5 mL of a 1 : 1 EtOH/H$_2$O mixture was added to a stirred solution of YCl$_3$·6H$_2$O (0.10 g, 0.33 mmol) in water (4 mL). Instantly, a colourless precipitate was produced. Stirring was continued for a further 2 h, then the reaction mixture was filtered. The colourless residue was washed with H$_2$O (2 × 5 mL) and hot EtOH (2 × 5 mL) to yield [Y(mbp)$_3$(H$_2$O)] (0.19 g, 85 %) upon drying as a colourless powder, mp 134–136°C. TGA weight loss calculated for one H$_2$O: 2.64 %. Found in the range of 80–130°C: 2.52 %. ν_{max} (neat)/cm^{-1} 3486wbr, 3027vw, 2915wbr, 1695m, 1678m, 1589s, 1557s, 1433s, 1399s, 1356m, 1297m, 1256w, 1239m, 1218w, 1202m, 1179m, 1110w, 1080w, 1063w, 1038w, 1018w, 994w, 976w, 950w, 890w, 857w, 838w, 817s, 810s. δ_H ([D$_6$]dmso, 400.17 MHz) 2.35 (9H, s, C*H*$_3$), 2.39 (6H, t, C*H*$_2$COO), 3.11 (6H, t, C*H*$_2$CO), 7.28 (6H, d, Ar *m-H*), 7.84 (6H, d, Ar *o-H*). δ_H (D$_2$O, 400.17 MHz) 2.37 (9H, s, C*H*$_3$), 2.52 (6H, t, C*H*$_2$COO), 3.27 (6H, t, C*H*$_2$CO), 7.36 (6H, d, Ar *m-H*), 7.87 (6H, d, Ar *o-H*). δ_C ([D$_6$]dmso, 75 MHz) 21.2, 30.6, 33.8, 56.1, 128.0, 129.2, 134.4, 143.3, 182.9br, 198.8. Found: C 58.12, H 5.16, Y 13.13. C$_{33}$H$_{35}$YO$_{10}$ (680.54) requires C 58.24, H 5.18, Y 13.06 %.

[La(mbp)$_3$(H$_2$O)]

Method A: Similarly to the synthesis protocol used for [Y(mbp)$_3$(H$_2$O)], the reaction between Na(mbp) (0.21 g, 0.98 mmol) and LaCl$_3$·6H$_2$O (0.12 g, 0.33 mmol) yielded [La(mbp)$_3$(H$_2$O)] (0.20 g, 85 %) upon drying as a colourless powder.

Method B: [La(O$_2$CCH$_3$)$_3$]·H$_2$O (0.11 g, 0.35 mmol) in 3 : 1 EtOH/H$_2$O was treated with an EtOH solution of Hmbp (0.21 g, 1.13 mmol), resulting in formation of a colourless precipitate, which was washed with H$_2$O (5 mL) and EtOH (2 × 5 mL) and dried in a desiccator to yield [La(mbp)$_3$(H$_2$O)] as a colourless powder (0.20 g, 83 %), mp 194–195°C. TGA weight loss calculated for one H$_2$O: 2.46 %. Found: 1.51 %. ν_{max} (neat)/cm^{-1} 3514wbr, 3463wbr, 3058vw, 3026vw, 2913wbr, 1683m, 1670m, 1605m, 1572m, 1551s, 1531s, 1518m, 1431s, 1405s, 1356m, 1300w, 1240m, 1200m, 1186m, 781w, 976w, 950w, 890m, 863w, 845w, 812s, 787w, 684w, 654w. δ_H ([D$_6$]dmso, 400.17 MHz) 2.35 (9H, s, C*H*$_3$), 2.37 (6H, t, C*H*$_2$COO), 3.09 (6H, t, C*H*$_2$CO), 7.28 (6H, d, Ar *m-H*), 7.83 (6H, d, Ar *m-H*). δ_C([D$_6$]dmso, 75 MHz) 21.5, 31.8, 34.3, 128.3, 129.5, 134.8, 143.5, 183.3, 199.2 ppm. Found: C 53.98, H 4.93, La 19.13. C$_{33}$H$_{35}$LaO$_{10}$ (730.54) requires C 54.26, H 4.83, La 19.01 %.

[Ce(mbp)$_3$(H$_2$O)]

Method A: Similarly to the synthesis protocol used for [Y(mbp)$_3$(H$_2$O)], the reaction between Na(mbp) (0.21 m, 0.97 mmol) and CeCl$_3$·7H$_2$O (0.12 g, 0.32 mmol) yielded [Ce(mbp)$_3$(H$_2$O)] (0.19 g, 80 %) upon drying as a colourless powder.

Method B: Similarly to the synthesis protocol used for [La(mbp)$_3$(H$_2$O)] (Method B), the reaction between [Ce(O$_2$CCH$_3$)$_3$]·H$_2$O (0.16 g, 0.46 mmol) and Hmbp (0.263 g, 1.37 mmol) yielded [Ce(mbp)$_3$(H$_2$O)] as a colourless powder (0.25 g, 73 %), mp 146–148°C. TGA weight loss calculated for one H$_2$O: 2.47 %. Found in the range of 80–130°C: 2.31 %. ν_{max} (neat)/cm^{-1} 3455 wbr, 3068w, 3027vw, 2952vw, 2913wbr, 1695m, 1675m, 1630w, 1607m, 1572m, 1542s, 1423m, 1400s, 1356s, 1300m, 1268w, 1240m, 1203m, 1179m, 1148w, 1110w, 1078w, 1062w, 1040vw, 1011w, 991w, 970m, 894m, 884w, 855w, 842w, 810s, 789s, 728w, 677w, 657w. δ_H ([D$_6$]dmso, 400.17 MHz) 2.35 (9H, s, C*H*$_3$), 3.95 (12H, vbr, C*H*$_2$), 7.32 (6H, br, Ar *m-H*), 8.01 (br, 6H, Ar *o-H*). δ_C([D$_6$]dmso, 75 MHz) 21.1, 34.5br, 128.0, 129.2, 134.7, 143.1, 199.3 (*C*OOCe and *C*H$_2$COO signals were not observed). Found: C 54.06, H 4.85, Ce 19.33. C$_{33}$H$_{35}$CeO$_{10}$ (731.75) requires C 54.17, H 4.82, Ce 19.15 %. Single crystals of [Ce(mbp)$_3$(H$_2$O)] were grown from a reaction mixture filtrate over several months and single crystals of [Ce(mbp)$_3$(dmso)] were grown from a saturated solution of [Ce(mbp)$_3$(H$_2$O)] in dmso.

[Nd(mbp)$_3$(H$_2$O)]

Method A: Similarly to the synthesis protocol used of [Y(mbp)$_3$(H$_2$O)], the reaction between Na(mbp) (0.12 g, 0.55 mmol) and NdCl$_3$·6H$_2$O (0.066 g, 0.18 mmol) yielded [Nd(mbp)$_3$(H$_2$O)] (0.087 g, 65 %) upon drying as a colourless powder.

Method B: Similarly to the synthesis protocol used for [La(mbp)$_3$(H$_2$O)] (Method B), the reaction between [Nd(O$_2$CCH$_3$)$_3$]·H$_2$O (0.10 g, 0.29 mmol) and Hmbp (0.17 g, 0.87 mmol) yielded [Nd(mbp)$_3$(H$_2$O)] as a colourless powder (0.14 g, 66 %), mp 178–180°C. TGA weight loss calculated for one H$_2$O: 2.45 %. Found in the range of 80–130°C: 2.26 %. ν_{max} (neat)/cm^{-1} 3460wbr, 3027vw, 2915w, 2900w, 1693m, 1675m, 1631w, 1605m, 1576s, 1553s, 1428s, 1400s, 1357s, 1295s, 1264w, 1239m, 1217vw, 1202m, 1181s, 1149vw, 1109vw, 1018w, 970w, 957w, 946vw, 886w, 855w, 813m, 807s, 791m, 678w, 657m. δ_H ([D$_6$]dmso, 400.17 MHz) 2.35 (9H, s, C*H*$_3$), 4.35 (12H, vbr, C*H*$_2$), 7.37 (6H, d, Ar *m-H*), 8.14 (6H, br, Ar *o-H*). δ_C ([D$_6$]dmso, 75 MHz) 21.6, 38.5vbr, 128.6, 129.7, 135.2, 143.6, 199.9 (COONd and CH$_2$COO signals were not observed). Found: C 52.71, H 4.79, Nd 19.13. C$_{33}$H$_{35}$NdO$_{10}$ (735.88) requires C 53.86, H 4.82, Nd 19.60 %. Single crystals of [Nd(mbp)$_3$(H$_2$O)] were grown from a reaction filtrate over several months.

[Ho(mbp)$_3$(H$_2$O)]

Similarly to the synthesis protocol used for [Y(mbp)$_3$(H$_2$O)], the reaction between Na(mbp) (1.68 g, 7.92 mmol) and HoCl$_3$·6H$_2$O (1.00 g, 2.64 mmol) yielded [Ho(mbp)$_3$(H$_2$O)] as a light pink powder (1.72 g, 86 %), mp 154°C. TGA weight loss

calculated for one H_2O: 2.38 %. Found in the range of 80–130°C: 2.04 %. ν_{max} (neat)/cm^{-1}: 3482wbr, 2912wbr, 1692m, 1675m, 1587s, 1556s, 1432s, 1399s, 1356m, 1296m, 1239m, 1202m, 1179m, 971w, 890s, 857s. δ_H ([D_6]dmso, 400.17 MHz) 2.83 (9H, s, C*H*$_3$), 8.03 (6H, brs, *m-H*), 10.3 (6H, brs, *o*-H), 17.2 (too broad for a satisfactory integration, vbr, CH_2CO), 29.9 (too broad for satisfactory integration, v br, CH_2COO). δ_H(D_2O, 400.17 MHz) 2.46 (9H, s, CH_3), 3.43 (6H, br, CH_2COO), 3.76 (6H, br, CH_2CO), 7.28 (6H, br, Ar *m-H*), 7.84 (6H, br, Ar *o-H*). Found: C 51.99, H 4.96, Ho 21.70. $C_{33}H_{35}HoO_{10}$ (756.56) requires C 52.39, H 4.66, Ho 21.80 %. Single crystals were grown in a H-tube, with the metathesis reactants in separate arms.

[Er(mbp)$_3$(H$_2$O)]

Similarly to the synthesis protocol used for [Y(mbp)$_3$(H_2O)], the reaction between Na(mbp) (1.68 g, 7.92 mmol) and $ErCl_3 \cdot 6H_2O$ (1.00 g, 2.62 mmol) yielded [Er(mbp)$_3$(H_2O)] (1.58 g, 79 %) as a light pink powder, mp 158°C. TGA weight loss calculated for one H_2O: 2.37 %. Found in the range of 80–130°C: 2.44 %. ν_{max} (neat)/cm^{-1} 3489wbr, 2942wbr, 1693m, 1676m, 1590s, 1557s, 1433s, 1399s, 1356m, 1296m, 1238m, 1202m, 1179m, 972w, 815s, 807s. δ_H([D_6]dmso, 400.17 MHz) −2.65 (~6H, vbr, CH_2COO), −0.13 (~6H, vbr, CH_2CO), 2.04 (9H, br, CH_3), 6.8–7.25 (12H, complex, Ar-*H*). δ_H (D_2O, 400.17 MHz) 2.26 (6H, br, CH_2COO), 2.38 (9H, brs, CH_3), 3.15 (6H, br, CH_2CO), 7.36 (6H, br, Ar *m-H*), 7.90 (6H, br, Ar *o-H*). Found: C 51.90, H 4.96, Er 21.80. $C_{33}H_{35}ErO_{10}$ (758.89) requires C 52.23, H 4.65, Er 22.04 %.

X-Ray Crystallography Data

All samples were coated in viscous oil and mounted in a cryostream on the respective diffractometers: a Bruker APEX II CCD diffractometer ([Ce(mbp)$_3$(dmso)]), with integration and absorption corrections completed using *Apex II* program suite,[23] and the MX1 ([Ho(mbp)$_3$(H_2O)]) and MX2 ([Ce(mbp)$_3$(H_2O)] and [Nd(mbp)$_3$(H_2O)]) macromolecular beamlines at the Australian Synchrotron, where the data and integration were completed by *Blu-ice*[24] and *XDS*[25] software programs, respectively. Structural solutions were obtained by Direct methods[26] and refined using full matrix least-squares methods against F2 using *SHELX97*[26] within the *OLEX 2*[27] interface. Collection temperatures and further details are supplied in the information below. Crystallographic data (excluding structure factors) for the structures reported in this paper have been deposited at the Cambridge Crystallographic Data Centre as supplementary numbers CCDC 1505758, 1505762, and 1505823. Copies of the data can be obtained free of charge on application to CCDC, 12 Union Road, Cambridge, CB2 1EZ, UK (fax: +44 (0) 1223 336033; email: deposit@ccdc.cam.ac.uk).

[Ce(mbp)$_3$(H$_2$O)]

$C_{33}H_{35}O_{10}Ce$, M 731.73 g mol^{-1}, colourless needle, 0.02 × 0.001 × 0.001 mm^3, monoclinic, space group $P2_1/c$ (no. 14), a 33.007(7), b 12.000(2), c 7.8650(16), β 92.49(3)°, V 3112.3(11) Å^3, Z 4, D_c 1.562 g cm^{-3}, T 100 K, μ 1.520 mm^{-1}, 48558 reflections measured (3.7° ≤ 2θ ≤ 54.46°), 6921 unique (R_{int} 0.0495, R_σ 0.0245) which were used in all calculations. The final R_1 was 0.0422 (>2σ(I)) and wR_2 was 0.1043 (all data). Refinement details: DFIX commands were used to model the hydrogen atoms on the water, with the bond distances set to 0.86 Å.

[Nd(mbp)$_3$(H$_2$O)]

$C_{33}H_{35}NdO_{10}$, M 735.85 g mol^{-1}, colourless needle, 0.02 × 0.001 × 0.001 mm^3, monoclinic, space group $P2_1/c$ (no. 14), a 33.007(7), b 12.000(2), c 7.8650(16), β 92.49(3)°, V 3112.3(11) Å^3, Z 4, D_c 1.570 g cm^{-3}, T 100 K, μ 1.726 mm^{-1}, 44512 reflections measured (2.46° ≤ 2θ ≤ 52.04°), 6105 unique (R_{int} 0.0685, R_σ 0.0335) which were used in all calculations. The final R_1 was 0.0651 (>2σ(I)) and wR_2 was 0.1528 (all data). Refinement details: crystals consistently grew as twinned needles. Even upon breaking off a very small piece for the analysis run using a synchrotron light source, some twinning of the data was observed leading to a large residual Q peak near the Nd site though after partially accounting for twinning using the TWIN command (BASF = 0.0146(9)), which significantly improved the model. DFIX commands were used to model the hydrogen atoms on the water, with the bond distances set to 0.86 Å.

[Ce(mbp)$_3$(dmso)]

$C_{35}H_{39}CeO_{10}S$, M 791.84 g mol^{-1}, colourless prism, 0.20 × 0.08 × 0.08 mm^3, monoclinic, space group $C2/c$ (No. 15), a 44.818(2), b 8.3296(4), c 18.5763(12) Å, β 105.075(6)°, V 6696.2(6) Å^3, Z 8, D_c 1.571 g cm^{-3}, F_{000} = 3224, Xcalibur, Ruby, Gemini ultra, Mo Kα radiation, λ 0.71073 Å, T 123(2) K, 2θ_{max} = 55.0°, 24577 reflections collected, 7666 unique (R_{int} = 0.0542). Final *GooF* 1.042, R_1 0.0368, wR_2 0.0707, R indices based on 5692 reflections with I > 2σ(I) (refinement on F^2), 429 parameters, 0 restraints. Lp and absorption corrections applied, μ 1.480 mm^{-1}.

Supplementary material

IR and NMR spectra are available on the Journal's website.

Acknowledgements

We acknowledge initial funding from the Australian Research Council through the Centre for Green Chemistry. The authors thank Dr Finlay Shanks for assistance with thermogravimetric analysis. Part of this work was undertaken on the MX1 and MX2 beamlines at the Australian Synchrotron, Victoria, Australia.[28] Powder XRD measurements were conducted using the facilities within the Monash X-ray Platform. CdeBD thanks the Australian government for the award of an Australian Postgraduate Award (APA). SH acknowledges support from the DAAD and the University of Leipzig.

References

[1] (a) J. Sinko, *Prog. Org. Coat.* **2001**, *42*, 267. doi:10.1016/S0300-9440(01)00202-8
(b) M. Forsyth, K. Wilson, T. Behrsing, C. Forsyth, G. B. Deacon, A. Phanasgoankar, *Corrosion* **2002**, *58*, 953. doi:10.5006/1.3280785

[2] M. Forsyth, M. Seter, B. Hinton, G. Deacon, P. Junk, *Aust. J. Chem.* **2011**, *64*, 812. doi:10.1071/CH11092

[3] (a) M. Costa, *Crit. Rev. Toxicol.* **1997**, *27*, 431. doi:10.3109/10408449709078442
(b) R. Codd, C. T. Dillon, A. Levina, P. A. Lay, *Coord. Chem. Rev.* **2001**, *216–217*, 537. doi:10.1016/S0010-8545(00)00408-2

[4] (a) B. R. W. Hinton, *J. Alloys Compd.* **1992**, *180*, 15. doi:10.1016/0925-8388(92)90359-H
(b) M. Bethencourt, F. J. Botana, J. J. Calvino, M. Marcos, M. A. Rodríguez-Chacón, *Corros. Sci.* **1998**, *40*, 1803. doi:10.1016/S0010-938X(98)00077-8

[5] (a) A. H. Ratten, P. H. Brook, R. D. Graham, D. E. Fribe, *Handbook on the Physics and Chemistry of Rare Earths* **1990**, Vol. 13, Ch. 92, pp. 423–451 (Elsevier: Amsterdam)
(b) Z. Hu, H. Richter, G. Sparovek, E. Schnug, *J. Plant Nutr.* **2004**, *27*, 183. doi:10.1081/PLN-120027555

[6] (a) M. L. He, U. Wehr, W. A. Rambeck, *J. Anim. Physiol. Anim. Nutr.* **2010**, *94*, 86. doi:10.1111/J.1439-0396.2008.00884.X
(b) H. M. L. U. Wehr, W. A. Rambeek, *Kraftfutter* **2006**, *89*, 16.
(c) W. Rambeck, U. Wehr, *Pig News and Information* **2005**, *26*, 41N.
[7] M. Forsyth, C. M. Forsyth, K. Wilson, T. Behrsing, G. B. Deacon, *Corros. Sci.* **2002**, *44*, 2651. doi:10.1016/S0010-938X(02)00024-0
[8] G. B. Deacon, C. M. Forsyth, T. Behrsing, K. Konstas, M. Forsyth, *Chem. Commun.* **2002**, 2820. doi:10.1039/B207722A
[9] G. B. Deacon, C. M. Forsyth, P. C. Junk, M. Hilder, S. G. Leary, C. Bromant, I. Pantenburg, G. Meyer, B. W. Skelton, A. H. White, *Z. Anorg. Allg. Chem.* **2008**, *634*, 91. doi:10.1002/ZAAC.200700359
[10] G. B. Deacon, M. Forsyth, P. C. Junk, S. G. Leary, W. W. Lee, *Z. Anorg. Allg. Chem.* **2009**, *635*, 833. doi:10.1002/ZAAC.200801379
[11] F. Blin, S. G. Leary, G. B. Deacon, P. C. Junk, M. Forsyth, *Corros. Sci.* **2006**, *48*, 404. doi:10.1016/J.CORSCI.2005.01.009
[12] N. D. Nam, A. Somers, M. Mathesh, M. Seter, B. Hinton, M. Forsyth, M. Y. J. Tan, *Corros. Sci.* **2014**, *80*, 128. doi:10.1016/J.CORSCI.2013.11.013
[13] G. B. Deacon, P. C. Junk, W. W. Lee, M. Forsyth, J. Wang, *New J. Chem.* **2015**, *39*, 7688. doi:10.1039/C5NJ00787A
[14] (a) M. Frey, S. G. Harris, J. M. Holmes, D. A. Nation, S. Parsons, P. A. Tasker, S. J. Teat, R. E. Winpenny, *Angew. Chem., Int. Ed.* **1998**, *37*, 3245. doi:10.1002/(SICI)1521-3773(19981217)37:23<3245::AID-ANIE3245>3.0.CO;2-F
(b) M. Frey, S. G. Harris, J. M. Holmes, D. A. Nation, S. Parsons, P. A. Tasker, R. E. Winpenny, *Chem. – Eur. J.* **2000**, *6*, 1407. doi:10.1002/(SICI)1521-3765(20000417)6:8<1407::AID-CHEM1407>3.0.CO;2-K
[15] (a) A. E. Somers, G. Talbi, C. N. de Bruin-Dickason, S. Hanf, M. Forsyth, G. B. Deacon, P. C. Junk, B. Hinton, in *Corrosion and Prevention 2016, ACA Conference, Auckland, NZ, 13–16 November* **2016**, (The Australian Corrosion Association: Kerrimuir, Vic.)
(b) A. E. Somers, G. Talbi, C. N. de Bruin-Dickason, M. Forsyth, G. B. Deacon, B. Hinton, in *NACE Corrosion 2016, Section 3,Vancouver, Canada, 6–10 March* **2016**, (NACE International: Houston, TX).
(c) A. E. Somers, G. B. Deacon, B. R. W. Hinton, D. R. MacFarlane, P. C. Junk, M. Y. I. Tan, M. Forsyth, *J. Indian Inst. Sci.*, in press.
[16] J. Marçalo, A. P. De Matos, *Polyhedron* **1989**, *8*, 2431. doi:10.1016/S0277-5387(89)80007-5
[17] R. Shannon, *Acta Cryst.* **1976**, *A32*, 751. doi:10.1107/S0567739476001551
[18] G. B. Deacon, T. Feng, P. C. Junk, B. W. Skelton, A. N. Sobolev, A. H. White, *Aust. J. Chem.* **1998**, *51*, 75. doi:10.1071/C97174
[19] G. B. Deacon, T. Feng, C. M. Forsyth, A. Gitlits, D. C. R. Hockless, Q. Shen, B. W. Skelton, A. H. White, *J. Chem. Soc., Dalton Trans.* **2000**, 961. doi:10.1039/A910277I
[20] G. B. Deacon, M. Forsyth, P. C. Junk, S. G. Leary, G. J. Moxey, *Polyhedron* **2006**, *25*, 379. doi:10.1016/J.POLY.2005.07.005
[21] T. Behrsing, G. B. Deacon, J. Luu, P. C. Junk, B. W. Skelton, A. H. White, *Polyhedron*, in press. doi:10.1016/j.poly.2016.05.047
[22] G. B. Deacon, R. J. Phillips, *Coord. Chem. Rev.* **1980**, *33*, 227. doi:10.1016/S0010-8545(00)80455-5
[23] F. Allen, *Acta Cryst.* **2002**, *B58*, 380. doi:10.1107/S0108768102003890
[24] T. M. McPhillips, S. E. McPhillips, H.-J. Chiu, A. E. Cohen, A. M. Deacon, P. J. Ellis, E. Garman, A. Gonzalez, N. K. Sauter, R. P. Phizackerley, S. M. Soltis, P. Kuhn, *J. Synchrotron Radiat.* **2002**, *9*, 401. doi:10.1107/S0909049502015170
[25] W. Kabsch, *J. Appl. Crystallogr.* **1993**, *26*, 795. doi:10.1107/S0021889893005588
[26] G. Sheldrick, *Acta Cryst.* **2008**, *A64*, 112. doi:10.1107/S0108767307043930
[27] O. V. Dolomanov, L. J. Bourhis, R. J. Gildea, J. A. K. Howard, H. Puschmann, *J. Appl. Crystallogr.* **2009**, *42*, 339. doi:10.1107/S0021889808042726
[28] N. P. Cowieson, D. Aragao, M. Clift, D. J. Ericsson, C. Gee, S. J. Harrop, N. Mudie, S. Panjikar, J. R. Price, A. Riboldi-Tunnicliffe, R. Williamson, T. Caradoc-Davies, *J. Synchrotron Radiat.* **2015**, *22*, 187. doi:10.1107/S1600577514021717